Inverse Compton scattering of coherent synchrotron radiation in an energy recovery linac

M. Shimada[1,*] and R. Hajima[2]

[1]*High Energy Accelerator Research Organization, KEK, Tsukuba, 305-0801, Japan*
[2]*Japan Atomic Energy Agency, Tokai, 319-1195, Japan*

(Received 22 June 2010; published 14 October 2010)

We propose inverse Compton scattering (ICS) of coherent synchrotron radiation (CSR) from a relativistic short electron bunch in energy recovery linacs (ERL) as a high-flux subpicosecond x-ray and γ-ray source. An advantage of the CSR scheme over a conventional ICS source is that no external laser is required, and synchronization between CSR pulses and electron bunches is obtained automatically. Moreover, higher-flux x rays can be generated from the ICS of CSR in an ERL operated at a high repetition rate, 100 MHz to 1.3 GHz. Using parameters of the Compact ERL at KEK, $1 \times 10^{13-14}$ phs/s b.w. 10% (the number of photons pulse^{-1} bandwidth unit^{-1}) x ray with a 100 fs–1 ps pulse duration can be obtained, for an energy range from 0.04 to 4 keV. In the case of a 5-GeV ERL, γ rays with energy around tens of MeV are generated with 1×10^8 phs/pulse b.w. 10% at a repetition rate of several hundreds of MHz.

DOI: 10.1103/PhysRevSTAB.13.100701 PACS numbers: 41.75.Lx, 07.85.Fv, 41.60.Ap, 42.60.Da

I. INTRODUCTION

Inverse Compton scattering (ICS), a process of photon scattering by relativistic electrons, can produce subpicosecond short-pulse, energy-tunable, quasimonochromatic x and γ rays. Generation of high-energy photons by ICS is now considered as a new class of light source after recent technological progress in high-power lasers and high-brightness electron beams.

A subpicosecond x ray is expected to open new phases in several scientific fields such as material, chemical, biological, and medical fields. Some projects of self-amplified spontaneous emission free-electron laser are now being undertaken for their use as a high-intensity x-ray source with short-pulse duration [1]. In storage rings, a special operation mode called the ''low alpha mode'' [2] and a technique called the ''laser bunch slicing'' [3] have been developed for a short-pulse x ray.

The ICS scheme is also a strong candidate for producing such short-pulse x rays [4]. Furthermore, a quasimonochromatic x ray is observed in ICS induced by free-electron laser (FEL) [5]. A high-brilliance x-ray photon source based on ICS with a superconducting linac is under development [6]. Gamma-ray sources based on ICS are also used regularly in nuclear physics [7]. Generation of a few tens of MeV γ rays from ICS is proposed for a polarized positron source for the International Linear Collider [8,9], nondestructive detection of nuclear materials [10], and photonuclear physics [11]. So far, such Compton sources have been developed by combining a high-energy electron accelerator and an external laser or a FEL driven by the same electron beam.

An energy recovery linac (ERL), which can accelerate small-emittance, short-pulse, and high-average current electron beams [12], is an ideal platform for ICS, because growth of emittance and energy spread due to the collision with photons are not issues in the ERL, in contrast to the storage rings. Here, we propose a scheme of high-energy photon generation from ICS of a subpicosecond electron bunch and coherent synchrotron radiation (CSR) in an ERL. In the proposed scheme, a subpicosecond electron bunch emits CSR in a terahertz (THz) or infrared wavelength region, and this CSR collides with a subsequent electron bunch to generate x rays. An advantage of the CSR scheme over a conventional ICS source is that no external laser is required and synchronization between CSR pulses and electron bunches is obtained automatically. Furthermore, high-flux x rays can be generated from CSR-ICS in an ERL operated at a high repetition rate, 100 MHz to 1.3 GHz.

II. COHERENT SYNCHROTRON RADIATION

When a bunch of relativistic electrons emits synchrotron radiation in a circular path, the radiation becomes coherent in the wavelength region $\lambda > \sigma_z$, where σ_z is the root mean square (rms) of the longitudinal bunch length. The spectral power of the CSR, $P(\lambda)$, is proportional to the square of the number of electrons in the bunch N_e [13,14]:

$$P(\lambda)d\lambda = [N_e + F(\lambda)N_e(N_e - 1)]p(\lambda)d\lambda, \qquad (1)$$

where $p(\lambda)$ is spectral power per electron. The form factor $F(\lambda)$ is defined using the longitudinal electron density $\lambda_e(z)$:

$$F(\lambda) = \left| \int \lambda_e(z) \exp\left[-i\frac{2\pi}{\lambda}z\right] dz \right|^2, \qquad (2)$$

where z is the longitudinal position from the reference particle. In the case of the longitudinal Gaussian beam with rms size σ_z, the longitudinal electron density is

*miho.shimada@kek.jp

written as $\lambda_e(z) = (1/\sqrt{2\pi}\sigma_z)\exp[-z^2/2\sigma_z^2]$; the spectrum of CSR is also Gaussian distribution as follows:

$$F(\lambda) = \exp[-(2\pi\sigma_z/\lambda)^2]. \quad (3)$$

The CSR spectrum from a subpicosecond electron bunch covers the THz range. The divergence of the CSR is given by

$$\Delta\theta_c = \left(\frac{3\lambda}{2\pi\rho}\right)^{1/3} = \frac{1}{\gamma}\left(\frac{2\lambda}{\lambda_c}\right)^{1/3}, \quad (4)$$

where λ_c, γ, and ρ are the critical wavelength, the Lorentz factor, and the curvature radius of the bending magnet.

III. INVERSE COMPTON SCATTERING

The ICS can be described as an undulator model when the electric field of an optical pulse is considered to be equivalent to a static magnetic field of an undulator. A schematic view of this optical undulator model is shown in Fig. 1. According to the undulator model, the central wavelength of the radiation photon λ_X can be described by the deflection parameter K and the undulator period λ_u as follows [4]:

$$\lambda_X = \frac{1}{2\gamma^2}\lambda_u\left(1 + \frac{K^2}{2}\right). \quad (5)$$

The number of photons per bunch N_X is

$$N_X \sim \pi\alpha K^2 N_e N_u, \quad (6)$$

where α and N_u are the fine structure constant and the number of undulator periods experienced by the electron.

In the case of an ICS scheme with head-on collisions of relativistic electrons, λ_u and N_u are replaced by the optical pulse parameters: $\lambda_u = \lambda/2$, $N_u = N_\lambda$, where N_λ is the number of optical cycle of the incident pulses. The deflection parameter K can be connected to the electric field of the optical pulse E_0 as in the following equation:

$$K = \frac{eE_0\lambda}{4\pi mc^2}, \quad (7)$$

where m and c are the electron rest mass and the velocity of light. In the case of CSR, the electric field at the collision point E_0 can be expressed as follows:

$$E_0 = \sqrt{\frac{2Z_0P(\lambda)(\Delta\lambda/\lambda)}{\sigma_t^{\mathrm{CSR}}\pi w_0^2}}, \quad (8)$$

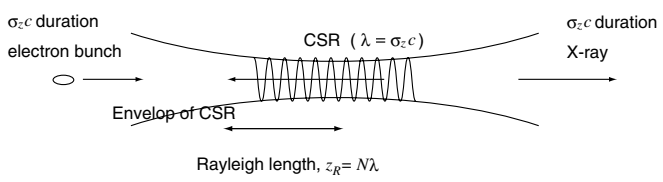

FIG. 1. Schematic drawing of the electron bunch and the laser envelop in inverse Compton scattering of coherent synchrotron radiation with a finite bandwidth.

where $Z_0(= 377\Omega)$, σ_t^{CSR}, and w_0 are the free-space impedance, the pulse duration of CSR, and the waist spot size at the collision point, respectively.

IV. SCHEMES OF OPTICS FOR COLLISION

In our proposed scheme, the CSR is used to generate x rays by ICS, as shown in Fig. 2. CSR from the leading electron bunch is collected by a mirror close to the bending magnet. The succeeding electron bunch collides with the CSR and emits x rays, whose pulse duration corresponds to the electron bunch length. We propose two layouts: one utilizes a ''magic mirror'' with a large acceptance angle to collect the CSR and the other utilizes an optical cavity to enhance the CSR power by pulse stacking.

A magic mirror, which is a perfect focusing metallic mirror for the circular orbit [15], is used to focus the CSR emitted from an electron bunch along a circular orbit. It allows us to reproduce the temporal profile and transverse size at the emission point if the cutoff frequency is negligible.

In the latter layout, the CSR power can be enhanced in an optical cavity equipped with mirrors of high reflectivity, such as multilayered mirrors or photonic crystal mirrors [16]. In a conventional optical cavity configuration, mode-locked laser pulses are stacked coherently after being injected from outside the optical cavity through the low-transmittance mirror [6,17]. On the other hand, the CSR pulses are emitted in the optical cavity and stacked incoherently. The intracavity optical power, $P_{\mathrm{CAV}}(\lambda)$, for the incoherent stacking after a large number of injections can be approximated as follows:

$$P_{\mathrm{CAV}}(\lambda) = \lim_{l\to\infty}\sum_{m=0}^{l} r^{mn}P(\lambda) = \frac{P(\lambda)}{1 - r^n(\lambda)}, \quad (9)$$

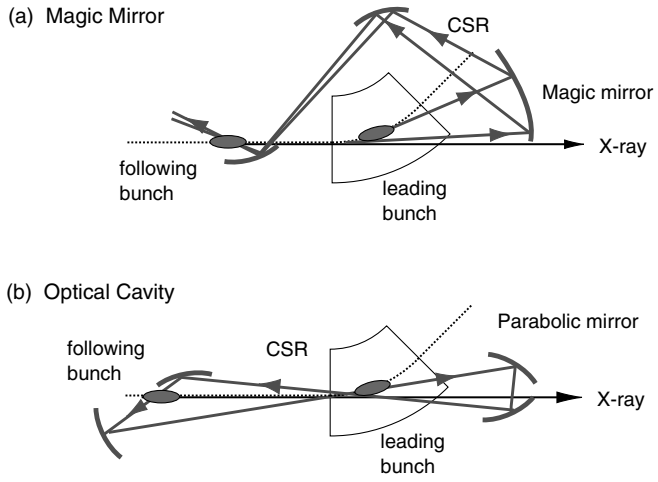

FIG. 2. Schematic drawing of the optics for inverse Compton scattering.

where $r(\lambda)$ and n are the reflectivity and the number of the mirrors in the optical cavity, respectively. In this case, $P(\lambda)$ in Eq. (8) should be replaced with $P_{\mathrm{CAV}}(\lambda)$.

Simultaneously, the acceptance angle to accumulate the entire CSR in the optical cavity is limited by the mode-matching condition, which is written as follows:

$$\sigma_x^{\mathrm{CSR}}\sigma_{x'}^{\mathrm{CSR}} \leq \frac{\lambda}{4\pi}, \tag{10}$$

where σ_x^{CSR} and $\sigma_{x'}^{\mathrm{CSR}}$ are the horizontal spread and divergence of the CSR source to the axis of the optical cavity, respectively. Each term on the left-hand side of Eq. (10) depends on the horizontal rms size σ_x and horizontal divergence $\sigma_{x'}$ of the electron bunch, the divergence of CSR $\Delta\theta_c$, and the bending angle Θ, written as follows:

$$\sigma_x^{\mathrm{CSR}} = \sqrt{\sigma_x^2 + \left[\rho\left(1-\cos\frac{\Theta}{2}\right)\right]^2} \tag{11}$$

$$\sigma_{x'}^{\mathrm{CSR}} = \sqrt{\sigma_{x'}^2 + \Delta\theta_c^2 + \left(\frac{\Theta}{2}\right)^2}. \tag{12}$$

The circular orbit of the electron in the optical cavity is schematically shown in Fig. 3. The maximum acceptance angle of the optical cavity configuration, $\Theta_C^{\max}$, is obtained by substituting Eqs. (11) and (12) into Eq. (10).

Moreover, the bandwidth of the CSR stored in the cavity is restricted by that of the high-reflectivity mirrors $\Delta\lambda$. If it is much less than λ, the number of the optical cycles increases to $\lambda/\Delta\lambda = N_\lambda$ and the CSR pulse duration σ_t^{CSR} in Eq. (8) is stretched as $N_\lambda\sigma_z/c$. The bandwidth of the high-reflectivity mirror $\Delta\lambda/\lambda$ is assumed to be close to 10%. For a head-on collision, the energy spread of the x rays is similar to $\Delta\lambda/\lambda$ in the typical beam parameter in ERL [18]. Details of the transverse and longitudinal electron beam size at the emission point are discussed in another paper [19].

When the CSR pulses are confined to the cavity's fundamental mode, the electric field can be expressed by a Gaussian beam [20]. The beam waist size w_0 is related to the Rayleigh length z_R as follows $\pi w_0^2 = \lambda z_R$. When $z_R = \lambda$, the electron collides with only one cycle of the CSR pulse with a small spot size, because the spot size increases rapidly when the electrons travel farther than the Rayleigh length λ from the focused point. Therefore we choose the Rayleigh length as $N_\lambda\lambda$ to collide the electron with N_λ cycles with the spot size as small as that of the focus point $N_\lambda\lambda^2$. The total number of on-axis scattered photons does not change by the lengthening of the Rayleigh length, because the effect due to the increase in the spot size is compensated by the increase in the number of CSR cycles. In such a condition, the higher quality x rays can be expected because the deflection parameter K and the divergence of the focused CSR are suppressed.

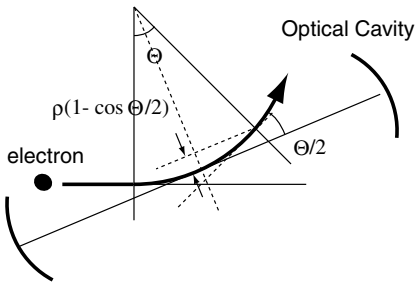

FIG. 3. Schematic of the orbit of the electron in the bending magnet equipped with the optical cavity.

V. PERFORMANCE OF X-RAY AND γ-RAY GENERATION AT ENERGY RECOVERY LINAC

Some performances of x rays and γ rays are shown using parameters of both Compact ERL and 5-GeV ERL. In the

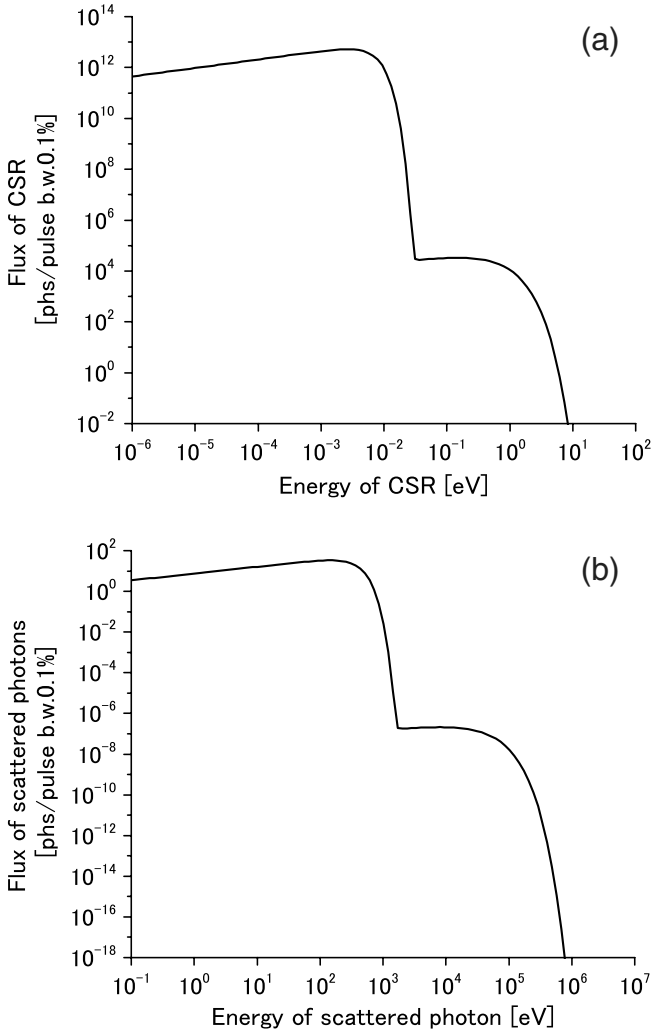

FIG. 4. Spectra of (a) CSR and (b) on-axis x ray in the case of magic mirror. Electron energy, bunch length σ_z, and electron charge is 60 MeV, 0.1 ps, and 77 pC/pulse, respectively. The horizontal acceptance angle is 300 mrad. The average of the transverse beam size over the orbit in the bending magnet is assumed to be 100×50 μm^2.

TABLE I. Optical cavity scheme in the Compact ERL: Horizontal acceptance angles are 50 mrad for $\lambda = 190$ μm and 110 mrad for $\lambda = 1900$ μm for mode matching. Bandwidth of the on-axis x ray is considered to be $\Delta\lambda_X/\lambda_X \sim \Delta\lambda/\lambda \sim 0.1$ (10%). Pulse duration of the x ray is the same as σ_z/c.

Electron energy [MeV]	Charge [nC]	σ_z/c [ps]	Spot size [mm × mm]	CSR energy [mJ]	K	X ray energy [keV]	N_X [phs/pulse]	N_X [phs/s]
60	0.077	0.1	0.3×0.3	0.14	0.013	0.4	1×10^4	2×10^{13}
60	0.5	1	3×3	0.6	0.009	0.04	4×10^4	0.7×10^{13}
200	0.2	0.1	0.3×0.3	1.0	0.034	4	2×10^5	1×10^{14}
200	1	1	3×3	2.5	0.017	0.4	3×10^5	3×10^{13}

TABLE II. Optical cavity scheme in 5-GeV ERL: Horizontal acceptance angles are 12 mrad for $\lambda = 60$ μm and 9 mrad for $\lambda = 20$ μm for mode matching. Bandwidth of the on-axis γ ray is considered to be $\Delta\lambda_\gamma/\lambda_\gamma \sim \Delta\lambda/\lambda \sim 0.1$ (10%). Pulse duration of the γ ray is the same as σ_z/c.

Electron charge [nC]	σ_z/c [fs]	Spot size [μm × μm]	CSR energy [mJ]	K	γ-ray energy [MeV]	N_γ [phs/pulse]	N_γ [phs/s]
1	30	100×100	80	0.56	8	3×10^8	3×10^{16}
0.5	10	30×30	65	0.87	25	4×10^8	0.7×10^{17}

case of Compact ERL, a curvature radius and bending angle of the bending magnet are 1 m and 45°, respectively. The maximum beam current is 100 mA. The electron beam parameters such as bunch charge, bunch duration, and transverse size are chosen taking into account the beam dynamics for a short electron bunch, such as the bunch compression, the CSR wake, and the space charge force.

An example of CSR spectrum in the ''magic mirror configuration'' and the on-axis scattered photons spectrum are shown in Fig. 4. The spot size of the focused CSR at the collision point is assumed to be the same as the mean value of the transverse size of the electron bunch at the emission point. The total number of scattered photons N_X is 2×10^5 phs/pulse (the number of photons pulse^{-1}). The flux is estimated to be 2×10^{14} phs/s (the number of photons s^{-1}) at the repetition rate of 1.3 GHz. The pulse duration of the scattered photons is the same as the electron bunch length σ_z, 100 fs. However, it can be stretched when we use a grating monochromator to obtain an x ray of narrow bandwidth.

In the case of the optical cavity equipped with four high-reflectivity mirrors of 99.98%, the intensity of CSR can be amplified by almost 1000 times. According to Eq. (3), the center wavelength of $\lambda = 2\pi\sigma_z$ is appropriate for stacking CSR in the optical cavity. Some examples of the performances are listed in Table I. The on-axis photons 10^{4-5} phs/pulse and 10^{13-14} phs/s in all cases are obtained within the bandwidth of 10%. The number of x-ray photons for the lower electron energy (60 MeV) is less than that of the higher energy (200 MeV) because of the difficulties in the bunch compression for the lower energy. Comparing the two results with the same x-ray energy of 0.4 keV, the flux of the x-ray photons at the first line in Table I is almost the same as that at the fourth line. It can be explained by the fact that the increase in the flux due to large electron charge at higher energy is compensated by the decrease in the flux due to the large spot size of CSR with longer wavelength.

CSR-ICS is also possible in a high-energy multi-GeV ERL for x-ray synchrotron radiation. In this case, we discuss only the configuration of the optical cavity. The curvature radius and bending angle are assumed to be 20 m and 3°, respectively. The maximum electron beam current is the same as the Compact ERL, 100 mA. We choose a parameter set of higher electron charge of 1 nC and shorter bunch length 30 fs compared to those of the Compact ERL, because the collective effect in the multi-GeV electron beam is smaller. The amplification of the optical cavity is also assumed to be 1000 times using the high-reflectivity mirror. The mean value of the transverse beam size at the emission point is smaller than the mean value of the spot size of focused CSR. Performances of the CSR-ICS in the 5-GeV ERL are summarized in Table II. We can expect MeV class γ rays with a number of photons of 10^8 phs/pulse and the flux 10^{16} phs/s in both cases. The number of photons is almost the same in both cases but the energy of γ rays is higher at the shorter electron bunch.

VI. SUMMARY

To produce subpicosecond x rays and γ rays with high repetition rate, we proposed ICS using CSR instead of an external laser. In the magic mirror configuration, we showed CSR spectra and the scattered photons. In the optical cavity configuration, we presented possible performances of the x-ray and γ-ray generation at the Compact ERL and 5-GeV ERL.

ACKNOWLEDGMENTS

We appreciate the useful comments of M. Yamamoto, Y. Honda, H. Sakai, K. Harada, and T. Miyajima (KEK). The support of Professor K. Oide (KEK), Professor N. Kumagai (SPring-8), Professor Y. Kobayashi and Associate Professor S. Sakanaka (KEK) is gratefully acknowledged.

[1] For example, J. Arthur, LCLS Conceptual Design Report No. SLAC-R-593, 2002.
[2] For example, J. Feikes *et al.*, in *Proceedings of the 10th European Particle Accelerator Conference, Edinburgh, Scotland, 2006* (EPS-AG, Edinburgh, Scotland, 2006), pp. 157–159.
[3] For example, R. W. Schoenlein *et al.*, Science **287**, 2237 (2000).
[4] For example, K.-J. Kim *et al.*, Nucl. Instrum. Methods Phys. Res., Sect. A **341**, 351 (1994).
[5] N. Sei *et al.*, Opt. Lett. **34**, 1843 (2009).
[6] K. Sakaue *et al.*, Rev. Sci. Instrum. **80**, 123304 (2009).
[7] For example, W. R. Weller *et al.*, Prog. Part. Nucl. Phys. **62**, 257 (2009).
[8] T. Oomori *et al.*, Phys. Rev. Lett. **96**, 114801 (2006).
[9] I. V. Pogorelsky *et al.*, Phys. Rev. ST Accel. Beams **3**, 090702 (2000).
[10] R. Hajima *et al.*, J. Nucl. Sci. Technol. **45**, 441 (2008).
[11] T. Tajima, Report on the ELI Science, 2009, pp. 1–18.
[12] For example, D. H. Bilderback *et al.*, New J. Phys. **12**, 035011 (2010).
[13] J. S. Nodvick and D. S. Saxon, Phys. Rev. **96**, 180 (1954).
[14] J. Schwinger, Phys. Rev. **75**, 1912 (1949).
[15] For example, R. Lopez-Delgado and H. Szwarc, Opt. Commun. **19**, 286 (1976).
[16] M. Tecimer *et al.*, Phys. Rev. ST Accel. Beams **13**, 030703 (2010).
[17] E. R. Crosson *et al.*, Rev. Sci. Instrum. **70**, 4 (1999).
[18] W. J. Brown and F. V. Hartemann, Phys. Rev. ST Accel. Beams **7**, 060703 (2004).
[19] M. Shimada *et al.*, KEK Report No. 2010-10, 2010.
[20] A. E. Siegman, *Lasers* (University Science Books, Mill Valley, CA, 1986).